



## Heavy flavour precision physics from $N_f = 2 + 1 + 1$ lattice simulations

A. Bussone<sup>a</sup>, N. Carrasco<sup>b</sup>, P. Dimopoulos<sup>d,a,\*</sup>, R. Frezzotti<sup>a</sup>, P. Lami<sup>c</sup>, V. Lubicz<sup>c</sup>, F. Nazzaro<sup>a</sup>, E. Picca<sup>c</sup>, L. Riggio<sup>c</sup>, G.C. Rossi<sup>a</sup>, F. Sanfilippo<sup>e</sup>, S. Simula<sup>b,c</sup>, C. Tarantino<sup>c</sup>

<sup>a</sup>Dipartimento di Fisica, Università di Roma “Tor Vergata”, Via della Ricerca Scientifica 1, 00173, Rome, Italy

<sup>b</sup>INFN, Sezione di Roma Tre, Via della Vasca Navale 84, I-00146 Rome, Italy

<sup>c</sup>Dipartimento di Fisica, Università Roma Tre, Via della Vasca Navale 84, I-00146 Rome, Italy

<sup>d</sup>Museo Storico della Fisica e Centro Studi e Ricerche “Enrico Fermi”, Compendio del Viminale, Piazza del Viminale 1, I-00184 Rome, Italy

<sup>e</sup>School of Physics and Astronomy, University of Southampton, SO17 1BJ Southampton, U.K.

### Abstract

We present precision lattice calculations of the pseudoscalar decay constants of the charmed sector as well as determinations of the bottom quark mass and its ratio to the charm quark mass. We employ  $N_f = 2 + 1 + 1$  dynamical quark gauge configurations generated by the European Twisted Mass Collaboration, using data at three values of the lattice spacing and pion masses as low as 210 MeV. Strange and charm sea quark masses are close to their physical values.

**Keywords:**  $D_{(s)}$ -decay constants,  $b$ -quark mass, Lattice QCD, ETMC

### 1. Introduction

Physical processes in the heavy quark sector offer the possibility to get some of the more stringent tests of the Standard Model and to search for possible footprints of New Physics dynamics, by directly challenging the unitarity constraints of the CKM matrix.

Lattice QCD has already entered the precision era as the accuracy of numerical computations is becoming comparable to that of experiments. For some of the relevant hadronic quantities in Flavour Physics the goal of per cent precision has been achieved. State-of-the-art lattice calculations involve  $O(a)$ -improved fermionic actions with  $N_f = 2, 2+1$  and  $2+1+1$  dynamical flavours with the smallest simulated pion masses being today at the physical point or slightly higher and employing three or more values of the lattice spacing. For a review with a critical evaluation of lattice results and averages, see [1]. First computations with four non-degenerate quark flavours including electromagnetic effects have also been presented recently [2].

Direct computations by many lattice collaborations have shown that the cutoff effects in the  $D$ -sector are small and under control. Moreover, considerable progress has been recently made in flavour physics at the  $b$  mass, with the help of both effective theories approaches and thanks to the implementation of some innovative methods. All these progresses have allowed the determination of a number of  $B$ -physics parameters (e.g.  $m_b$ ,  $f_B$  and  $f_{B_s}$ ) with controlled systematic uncertainties.

Lattice methods are an invaluable tool to obtain direct determinations of hadronic quantities relevant for the computation of many of the so called golden plated processes such as decay constants, form factors and bag parameters. For instance, the width of the  $D$  and  $D_s$  leptonic decays is given, to lowest order, by

$$\Gamma(D_{(s)} \rightarrow \ell \nu) = \frac{G_F^2 f_{D_{(s)}}^2 m_\ell^2 M_{D_{(s)}}}{8\pi} \left(1 - \frac{m_\ell^2}{M_{D_{(s)}}^2}\right)^2 |V_{cd(s)}|^2. \quad (1)$$

Thus lattice computations of the quantities  $f_D$  and  $f_{D_s}$  gives access to the determination of the CKM matrix elements,  $|V_{cd}|$  and  $|V_{cs}|$ , respectively, as in Eq. (1) all the

\*Corresponding author, dimopoulos@roma2.infn.it

rest is known experimentally. On the experimental side also the accuracy of the measurements of the  $D$  [3, 4, 5] and  $D_s$  [6, 7] leptonic width has progressively improved during the years.

Lattice QCD provides a first principles' way to compute quark masses. This is possible since quark masses enter as parameters in the QCD Lagrangian and their values can be extracted by matching hadron masses calculated on the lattice with their experimental values. The accuracy of quark mass estimates depends on the conversion from the lattice regularisation to continuum renormalisation schemes. Quark mass ratios instead can be computed in a fully non-perturbative way and are free of renormalisation scheme ambiguities. We notice, here, that the knowledge of the  $b$ -quark mass value and to less extent that of the  $c$ -quark mass plays an important rôle in the study of the Higgs decay to  $b\bar{b}$  and  $c\bar{c}$  [8].

The European Twisted Mass Collaboration (ETMC) has undertaken an extensive program of heavy quark physics calculations on the lattice using two and four dynamical flavours. Here we present the results of the computation of the  $D_{(s)}$  pseudoscalar meson decay constants (in the isospin symmetric limit) and the  $b$  to  $c$  quark mass ratio obtained using gauge configurations with  $N_f = 2 + 1 + 1$  dynamical quarks. The main (*preliminary*) results in these proceedings are

$$f_D = 208.7(5.2) \text{ MeV}, \quad f_{D_s} = 247.5(4.1) \text{ MeV}, \quad (2)$$

$$\frac{f_{D_s}}{f_D} = 1.186(21), \quad \left( \frac{f_{D_s}}{f_D} \right) / \left( \frac{f_K}{f_\pi} \right) = 0.998(14), \quad (3)$$

$$m_b(\overline{\text{MS}}, m_b) = 4.26(16) \text{ GeV}, \quad (4)$$

$$m_b/m_c = 4.40(8) \quad (5)$$

For completeness we remind the recent ETMC determinations of the  $c$ -quark mass and the charm to strange quark mass ratio published in [9]:

$$m_c(\overline{\text{MS}}, m_c) = 1.348(42) \text{ GeV}, \quad m_c/m_s = 11.62(16) \quad (6)$$

For a preliminary ETMC computation of the  $B$ -meson decay constants, giving  $f_B = 196(9) \text{ MeV}$ ,  $f_{B_s} = 235(9) \text{ MeV}$  and  $f_{B_s}/f_B = 1.201(25)$ , we refer to [10].

## 2. Lattice setup

ETMC has produced gauge configurations with  $N_f = 2 + 1 + 1$  dynamical quarks [11] employing the Iwasaki gluon action [12] and the Wilson Twisted Mass fermionic action for the sea quarks [13]. Automatic  $O(a)$ -improvement is guaranteed both for the light and heavier quarks by tuning at maximal twist whilst the

drawback of the mixing between the strange and charm sectors [14] is avoided in the valence by using the Osterwalder-Seiler fermions [15]. We have data ensembles at three values of the lattice spacing in the range  $[0.06, 0.09] \text{ fm}$ . Simulated pion masses lie in the interval  $[210, 440] \text{ MeV}$ . Thanks to the properties of the twisted mass action light quarks in the sea and all types of quarks in the valence enjoy multiplicative mass renormalisation,  $Z_m = 1/Z_P$ , which is computed non-perturbatively using the RI'-MOM scheme [9]. Moreover owing to PCAC, at maximal twisted angle no normalisation constant is needed in the computation of the decay constants. In Ref. [9] we have presented our computation for the quark masses of the (degenerate) light  $m_{u/d}(\overline{\text{MS}}, 2 \text{ GeV}) = 3.70(17) \text{ MeV}$ , strange  $m_s(\overline{\text{MS}}, 2 \text{ GeV}) = 99.6(4.1) \text{ MeV}$  and charm  $m_c(\overline{\text{MS}}, m_c) = 1.348(42) \text{ GeV}$ , which are determined by using the experimental values of the pion, kaon and  $D$  (or  $D_s$ ) masses, respectively. The phenomenological value of  $f_\pi$  has been used for setting the scale.

In this work the computation of the decay constants in the charmed region as well as the determination of the  $b$ -quark mass are performed using (Gaussian) smearing meson operators [16, 17] combined with APE smeared links [18] in order to reduce both the coupling of the interpolating field with the excited states and the gauge noise of the links involved in the smeared fields. (For an alternative preliminary analysis of the charmed decay constants that use local point correlators see Ref.[19].) A summary of the most important details of our simulations is given in Table 1.

$\beta$	$V/a^4$	$a\mu_{\text{sea}} = a\mu_\ell$	$N_{\text{cfg}}$	$a\mu_s$	$a\mu_c - a\mu_h$
1.90	$32^3 \times 64$	0.0030	150	0.0180,	0.21256, 0.25000,
		0.0040	150	0.0220,	0.29404, 0.34583,
		0.0050	150	0.0260	0.40675, 0.47840,
1.90	$24^3 \times 48$	0.0040	150		0.56267, 0.66178,
		0.0060	150		0.77836,
		0.0080	150		
		0.0100	150		
1.95	$32^3 \times 64$	0.0025	150	0.0155,	0.18705, 0.22000,
		0.0035	150	0.0190,	0.25875, 0.30433,
		0.0055	150	0.0225	0.35794, 0.42099,
		0.0075	150		0.49515, 0.58237
1.95	$24^3 \times 48$	0.0085	150		0.68495,
2.10	$48^3 \times 96$	0.0015	90	0.0123,	0.14454, 0.17000,
		0.0020	90	0.0150,	0.19995, 0.23517,
		0.0030	90	0.0177	0.27659, 0.32531,
					0.38262, 0.45001,
					0.52928,

Table 1: Summary of simulation details. Gauge couplings  $\beta = 1.90, 1.95$  and  $2.10$  correspond to lattice spacings  $a = 0.089, 0.082$  and  $0.062$ , respectively; see Ref. [9]. We denote with  $a\mu_\ell$ ,  $a\mu_s$  and  $a\mu_c - a\mu_h$ , the light, strange-like, charm-like and somewhat heavier bare quark masses, respectively, entering in the valence sector computations.

### 3. Charmed decay constants

We use two point correlation functions with pseudoscalar interpolating operators,  $P(x) = \bar{q}_1(x)\gamma_5 q_2(x)$ , that in periodic lattice have the typical form:

$$C_{PP}(t) = (1/L^3) \sum_{\vec{x}} \langle P(\vec{x}, t) P^\dagger(\vec{0}, 0) \rangle$$

$$\xrightarrow{t \gg 0, (T-t) \gg 0} \frac{\xi_{PP}}{2M_{ps}} (e^{-M_{ps}t} + e^{-M_{ps}(T-t)}) \quad (7)$$

We take the Wilson parameters of the two valence quarks of the pseudoscalar meson to be opposite in order to guarantee that the cutoff effects on the pseudoscalar mass are  $O(a^2\mu)$  [21, 22, 23]. We then consider two cases, using smeared source only and source and sink both smeared. As for  $\xi_{PP}$ , this is given by  $\xi_{PP} = \langle 0|P^L|ps\rangle\langle ps|P^S|0\rangle$  in the first case and  $\xi_{PP} = \langle 0|P^S|ps\rangle\langle ps|P^S|0\rangle$  in the second one, where  $L$  and  $S$  indicate local and smeared operators. By combining the two kinds of correlators it is easy to obtain the matrix element of the local operator  $g_{ps} = \langle 0|P^L|ps\rangle$  which serves for computing the pseudoscalar decay constant (via PCAC) given by:

$$f_{ps} = (\mu_1 + \mu_2) \frac{g_{ps}}{M_{ps} \sinh M_{ps}}, \quad (8)$$

where  $\mu_{1,2}$  are the masses of the valence quarks that form the pseudoscalar meson with mass  $M_{ps}$ . The use of  $\sinh M_{ps}$  (rather than  $M_{ps}$ ) in Eq. (8) is beneficial for reducing the discretisation errors. For the computation of  $f_{D_s}$  we tune, via well controlled interpolations, one of the valence quark masses to the value of the strange mass and the other to the value of the charm mass, both taken from Ref. [9]. In this way, for each value of the sea light quark mass and of the three lattice spacings, we get estimates for the decay constant  $f_{cs}$ . Then a simultaneous extrapolation to the physical value of the  $u/d$  quark mass and to the continuum limit can be performed in order to obtain  $f_{D_s}$ . In the present analysis we consider the quantity  $(f_{cs}/M_{cs}) \times M_{D_s}^{expt}$ , where  $M_{cs}$  is a pseudoscalar meson mass made of  $c$  and  $s$  quarks and is computed at each value of the sea light quark mass, while  $M_{D_s}^{expt} = 1969.0(1.4)$  MeV is the experimental value of the  $D_s$  mass. The above choice of observable is advantageous because, first, in the determination of  $f_{D_s}$  any scale setting uncertainty is avoided and, second, this quantity presents very small discretisation effects. The fit ansatz of the combined chiral and continuum extrapolation reads:  $[(f_{cs}/M_{cs}) \times M_{D_s}^{expt}] = C_0 + C_1 \bar{\mu}_\ell + D a^2$ , see Fig. 1. We control chiral fit uncertainties by adding in the above fit ansatz either a quadratic quark mass term or

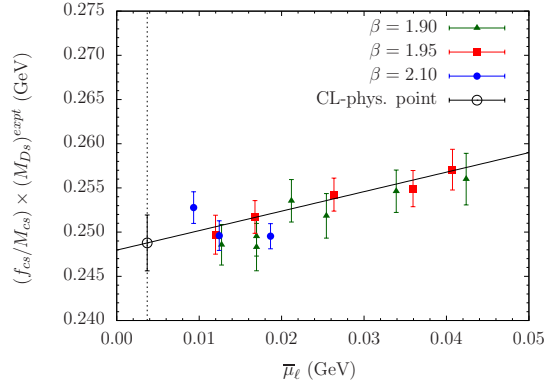


Figure 1: Combined chiral and continuum fit ( $\chi^2/(dof) = 0.8$ ) of  $(f_{cs}/M_{cs}) \times M_{D_s}^{expt}$  against the renormalised light quark mass expressed in  $\overline{\text{MS}}$ -scheme at the scale of 2 GeV,  $\bar{\mu}_\ell = \bar{\mu}_{sea}$ . The fit ansatz is linear both in  $\bar{\mu}_\ell$  and in  $a^2$ . The vertical black thin line marks the position of  $u/d$  quark mass point. The empty black circle is our result at the physical  $u/d$  quark mass point in the continuum limit.

fitting data corresponding to light pseudoscalar masses with  $M_{\ell\ell} < 350$  MeV. Finite volume systematics are estimated by fitting data corresponding to  $L > 2.6$  fm. Discretisation systematic errors have been estimated by fitting data either from the two finest lattice spacings or from the two coarsest ones, and also by estimating the difference of our results from the finest lattice to the continuum limit. Moreover, we have also included the propagated error due to the  $m_{s,c}$  uncertainties as well as the systematic effect of the quark mass renormalisation constant (RC) computed in two ways that differ by  $O(a^2)$  effects. Our central value is the weighted average over the results from all the analyses described above. Our (*preliminary*) result for  $f_{D_s}$  reads

$$f_{D_s} = 247.5(3.0)_{stat+fit}(2.7)_{syst}[4.1] \text{ MeV}, \quad (9)$$

where we report in square brackets the total error ( $\sim 1.6\%$ ) that is the sum in quadrature of the statistical and systematic uncertainties. For the full error budget see Table 2.

In Fig. 2 we compare our result with those computed in other lattice studies and with the PDG estimate based on experimental results and unitarity assumptions. Some tension between the PDG estimate and the most precise lattice results is still present.

In order to determine the SU(3) symmetry breaking ratio  $f_{D_s}/f_D$  we measure on our data sets the double ratio  $\mathcal{R}_f = (f_{cs}/f_{ct})(f_{\ell\ell}/f_{s\ell})$ . This choice enjoys the property of very mild light quark mass dependence as

uncertainty (in %)	$f_{D_s}$	$f_{D_s}/f_D$	$f_D$
stat. + fit	1.2	0.8	1.6
syst. from chiral fits	0.8	0.8	1.1
syst. from discr. effects	0.8	0.7	1.0
syst. from FSE	0.1	0.4	0.4
syst. from $f_K/f_\pi$	-	1.2	1.2
Total	1.6	1.8	2.5

Table 2: Full error budget for  $f_{D_s}$ ,  $f_{D_s}/f_D$  and  $f_D$ . The different sources of uncertainty are self explanatory.

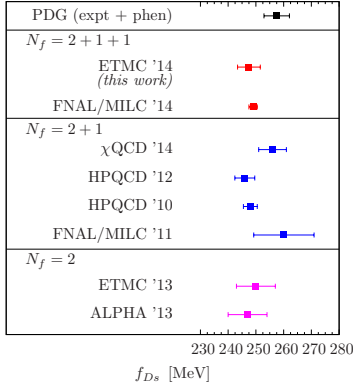


Figure 2: We compare the available continuum limit determinations for  $f_{D_s}$  (in MeV) from lattice studies that use  $N_f = 2, 2+1$  and  $2+1+1$  dynamical flavours. "ETMC '14" result refers to the present work. For the results of other lattice studies we refer to (from top to bottom) [24, 25, 26, 27, 28, 29, 30]). For the PDG result see [31].

expected from the large cancellation between the SU(2) chiral logarithms [32, 33]. The quantity  $\mathcal{R}_f$  in the continuum limit and at the physical pion mass point multiplied with  $(f_K/f_\pi)$  (taken from Ref. [20]) will provide the result for  $f_{D_s}/f_D$ . We try the following fit ansätze:

$$\mathcal{R}_f = c_0^{(1)} + c_1^{(1)}\bar{\mu}_\ell + D^{(1)}a^2, \quad (10)$$

$$\mathcal{R}_f = c_0^{(2)} \left[ 1 + c_1^{(2)}\bar{\mu}_\ell + \left( \frac{9\hat{g}^2}{4} - \frac{1}{2} \right) \xi_\ell \log \xi_\ell \right] + D^{(2)}a^2, \quad (11)$$

where  $\xi_\ell = (2B_0\bar{\mu}_\ell)/(4\pi f_0)^2$  with  $B_0$  and  $f_0$  determined in Ref. [9]. We have applied finite size corrections using Ref.[34]. Among the available estimates for the  $(D^*\pi)$  coupling we have used  $\hat{g} = 0.61(7)$  that in our case leads to the most conservative estimate for the chiral fit systematic uncertainty. The chiral and continuum limit extrapolation is shown in Fig. 3. Moreover we have performed an analysis similar to the one for  $f_{D_s}$  in order to estimate our systematic uncertainties. The full error budget is given in Table 2. The central value corresponds to the weighted average over results from all the

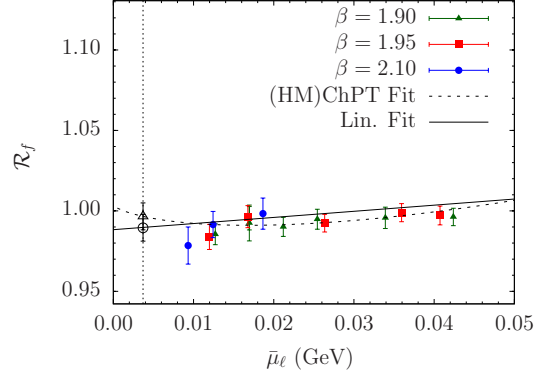


Figure 3: Combined chiral and continuum fit for the quantity  $\mathcal{R}_f$  against the renormalised light quark mass expressed in  $\overline{\text{MS}}$ -scheme at the scale of 2 GeV,  $\bar{\mu}_\ell = \bar{\mu}_{\text{sea}}$ . The vertical black thin line marks the position of  $u/d$  quark mass point. The empty black circle and empty triangle represent the results for the ratio  $f_{D_s}/f_D$ , using the fit ansatz of Eq. (10) ( $\chi^2/(dof) = 0.7$ ) and Eq. (11) ( $\chi^2/(dof) = 1.1$ ), respectively, at the physical  $u/d$  quark mass point and in the continuum limit.

different analyses. Our (*preliminary*) results read

$$(f_{D_s}/f_D)/(f_K/f_\pi) = 0.998(8)_{\text{stat+fit}}(11)_{\text{syst}}[14], \quad (12)$$

$$f_{D_s}/f_D = 1.186(9)_{\text{stat+fit}}(19)_{\text{syst}}[21], \quad (13)$$

and each one of the total errors (in square brackets) is the sum in quadrature of the statistical error and the systematic one.

We combine the results from Eqs. (9) and (13) to get our (*preliminary*) result for the decay constant of the  $D$ -meson, namely  $f_D = f_{D_s}/(f_{D_s}/f_D)$ , which reads:

$$f_D = 208.7(3.3)_{\text{stat+fit}}(4.0)_{\text{syst}}[5.2] \text{ MeV}, \quad (14)$$

where also in this case the total error written in square brackets ( $\sim 2.5\%$ ) is the sum in quadrature of the statistical and systematic uncertainties. For the complete error budget see Table 2.

In Figs. 4 and 5 we present a world comparison between lattice results for  $f_{D_s}/f_D$  and  $f_D$ , respectively. In both figures the PDG estimate is also included. For some recent non-lattice estimates of the charmed decay constants, see Refs. [35, 36, 37, 38].

#### 4. Computation of $m_b$ and $m_b/m_c$

We perform the determination of the  $b$ -quark mass employing the *ratio method* described in detail in Refs. [30, 39, 40]. We present here a variant of this

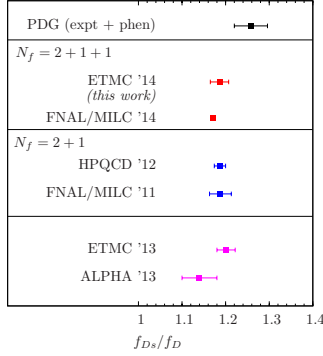


Figure 4: We compare the available continuum limit determinations for  $f_{Ds}/f_D$  from lattice studies that use  $N_f = 2, 2+1$  and  $2+1+1$  dynamical flavours. "ETMC '14" result refers to the present work. For the results of the other lattice studies we refer to (from top to bottom) [24, 26, 28, 29, 30]). For the PDG result see [31].

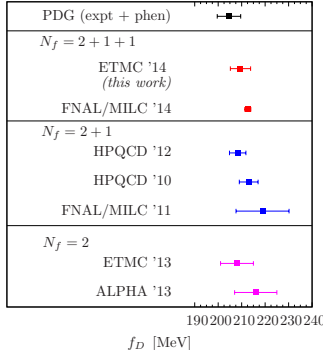


Figure 5: We compare the available continuum limit determinations for  $f_D$  (in MeV) from lattice studies that employ  $N_f = 2, 2+1$  and  $2+1+1$  dynamical flavours. "ETMC '14" result refers to the present work. For the results of the other lattice studies we refer to (from top to bottom) [24, 25, 26, 27, 28, 29, 30]). For the PDG result see [31].

method and we build the quantity  $Q_h = M_{hs}/(M_{hl})^\gamma$ , where  $M_{hs}$  and  $M_{hl}$  are the heavy-strange and heavy-light pseudoscalar masses, respectively. The parameter  $\gamma$  is a free one and may take values at will in the interval  $[0, 1)$ . By HQET arguments we know that for the asymptotic behaviour we get:

$$\lim_{\mu_h^{\text{pole}} \rightarrow \infty} \left( \frac{M_{hs}/(M_{hl})^\gamma}{(\mu_h^{\text{pole}})^{(1-\gamma)}} \right) = \text{const.}, \quad (15)$$

where  $\mu_h^{\text{pole}}$  is the heavy quark pole mass. We then consider a sequence of heavy quark masses expressed in the  $\overline{\text{MS}}$ -scheme at the scale of 2 GeV such that any two successive masses have a common and fixed ratio i.e.  $\bar{\mu}^{(n)} = \lambda \bar{\mu}^{(n-1)}$ ,  $n = 2, 3, \dots$ . The next step is to construct at each value of the sea quark mass and the lattice

spacing the following ratios:

$$\begin{aligned} y_Q(\bar{\mu}_h^{(n)}, \lambda; \bar{\mu}_\ell, \bar{\mu}_s, a) &\equiv \\ &\equiv \frac{Q_h(\bar{\mu}_h^{(n)}; \bar{\mu}_\ell, \bar{\mu}_s, a)}{Q_h(\bar{\mu}_h^{(n-1)}; \bar{\mu}_\ell, \bar{\mu}_s, a)} \cdot \left( \frac{\bar{\mu}_h^{(n)} \rho(\bar{\mu}_h^{(n)}, \mu^*)}{\bar{\mu}_h^{(n-1)} \rho(\bar{\mu}_h^{(n-1)}, \mu^*)} \right)^{(\gamma-1)} \\ &= \lambda^{(\gamma-1)} \frac{Q_h(\bar{\mu}_h^{(n)}; \bar{\mu}_\ell, \bar{\mu}_s, a)}{Q_h(\bar{\mu}_h^{(n)} / \lambda; \bar{\mu}_\ell, \bar{\mu}_s, a)} \left( \frac{\rho(\bar{\mu}_h^{(n)}, \mu^*)}{\rho(\bar{\mu}_h^{(n)} / \lambda, \mu^*)} \right)^{(\gamma-1)} \end{aligned} \quad (16)$$

with  $n = 2, 3, \dots$  and we have used the relation  $\mu_h^{\text{pole}} = \rho(\bar{\mu}_h, \mu^*) \bar{\mu}_h(\mu^*)$  between the  $\overline{\text{MS}}$  renormalised quark mass (at the scale of 2 GeV) and the pole quark mass. The  $\rho$ 's are known perturbatively up to  $\text{N}^3\text{LO}$ . For each pair of heavy quark masses we then carry out a simultaneous chiral and continuum fit of the quantity defined in Eq. (16) to obtain  $y_Q(\bar{\mu}_h) \equiv y_Q(\bar{\mu}_h, \lambda; \bar{\mu}_{u/d}, \bar{\mu}_s, a = 0)$ . By construction this quantity involves (double) ratios of pseudoscalar meson masses at successive values of the heavy quark mass, so we expect that discretisation errors will be under control. In fact this is the case even for the largest values of the heavy quark mass used in this work, see Fig. 6. Since we have taken into account the matching of QCD onto HQET concerning the evaluation of a heavy-light pseudoscalar mass,  $M_{hs/\ell}$ , our ratio  $y_Q(\bar{\mu}_h)$  has been defined in such a way that the following ansatz is sufficient to describe the  $\bar{\mu}_h$ -dependence<sup>1</sup>

$$y_Q(\bar{\mu}_h) = 1 + \frac{\eta_1}{\bar{\mu}_h} + \frac{\eta_2}{\bar{\mu}_h^2}, \quad (17)$$

in which the constraint  $\lim_{\bar{\mu}_h \rightarrow \infty} y_Q(\bar{\mu}_h) = 1$  has already been incorporated. This fit is reported in Fig. 7. Finally, we compute the  $b$ -quark mass via the *chain* equation

$$\begin{aligned} y_Q(\bar{\mu}_h^{(2)}) y_Q(\bar{\mu}_h^{(3)}) \dots y_Q(\bar{\mu}_h^{(K+1)}) &= \\ = \lambda^{K(\gamma-1)} \frac{Q_h(\bar{\mu}_h^{(K+1)})}{Q_h(\bar{\mu}_h^{(1)})} \cdot \left( \frac{\rho(\bar{\mu}_h^{(K+1)}, \mu^*)}{\rho(\bar{\mu}_h^{(1)}, \mu^*)} \right)^{\gamma-1} \end{aligned} \quad (18)$$

in which the values of the factors in the (lhs) are evaluated using the result of the fit function (Eq. 17) and  $\lambda$ ,  $K$  (integer) and  $\bar{\mu}_h^{(1)}$  are such that the quantity  $Q_h(\bar{\mu}_h^{(K+1)})$  matches  $M_{Bs}/(M_B)^\gamma$ , where  $M_{Bs} = 5366.7(4)$  MeV and  $M_B = 5279.3(3)$  MeV are the experimental values of the  $B_s$ - and  $B$ -meson masses [31], respectively. Notice that the quantity  $Q_h(\bar{\mu}_h^{(1)})$  for *any* value of  $\bar{\mu}_h^{(1)}$  around the charm quark mass is safely computed in the continuum limit and at the physical pion mass. For instance, using quark mass RC of the M2-type (see [9])

<sup>1</sup>For more details on this point see the Appendix of Ref. [40] and [30], section 4.

and setting as input  $\bar{\mu}_h^{(1)} = 1.148$  GeV and  $\gamma = 0.75$  we find  $(\lambda, K) = (1.1588, 10)$ . Thus, the  $b$ -quark mass in the  $\overline{\text{MS}}$ -scheme at the scale of 2 GeV is given by  $\bar{\mu}_b = \lambda^K \bar{\mu}_h^{(1)}$ . Our *preliminary* result for the  $b$ -quark mass is given by the average over two estimates obtained using either M1 or M2-type quark mass RCs while their half difference is taken as an additional systematic error. This reads

$$m_b(\overline{\text{MS}}, m_b) = 4.26(7)_{\text{stat+fit}}(14)_{\text{syst}}[16] \text{ GeV}, \quad (19)$$

where the total error (in brackets) is the sum in quadrature of the statistical and the systematic ones. For a complete error budget we refer to Table 3. We have

uncertainty (in %)	$m_b$	$m_b/m_c$
stat+fit	1.6	1.4
syst. from lat. scale	2.6	-
syst. from discr. effects	0.7	0.7
syst. from ratios fits	1.1	0.7
syst. from chiral fits	0.4	0.4
syst. from RC	1.4	-
Total	3.6	1.8

Table 3: Full error budget for  $m_b$  and  $m_b/m_c$ . The different sources of uncertainty are self explanatory.

verified that for a large range of values of  $\gamma \in [0, 1)$  we get fully compatible final results<sup>2</sup> for  $m_b$ . The freedom of choosing  $\gamma$  allows for better control of systematic uncertainties stemming from discretisation effects and the fit ansatz Eq. (17).

Finally, the ratio method offers the advantage of determining the ratio  $m_b/m_c$  in a simple and fully non-perturbative way. By setting  $\bar{\mu}_h^{(1)} = \bar{\mu}_c$  we repeat the above ratio method analysis and we find

$$m_b/m_c = 4.40(6)_{\text{stat+fit}}(5)_{\text{syst}}[8] \quad (20)$$

A complete error budget is also reported in Table 3. In Figs. 8 and 9 we present a comparison between lattice results for  $m_b$  and  $m_b/m_c$ , respectively. For non-lattice estimate of  $m_b$  see [41].

### Acknowledgements

We are grateful to all members of ETMC for fruitful discussions. We acknowledge the CPU time provided by the PRACE Research Infrastructure under the project PRA067 at the Jülich and CINECA SuperComputing Centers, and by the agreement between INFN and CINECA under the specific initiative INFN-lqcd123.

<sup>2</sup>This systematic uncertainty has been included in the estimate called "syst. from ratios fits" of Table 3.

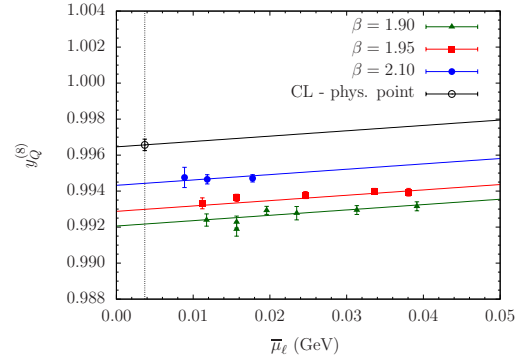


Figure 6: Combined chiral and continuum fit of the ratio defined in Eq. (16) and corresponding to the case of the two largest values of heavy quark mass against the renormalised light quark mass  $\bar{\mu}_\ell = \bar{\mu}_{\text{sea}}$ . The fit ansatz is linear both in  $\bar{\mu}_\ell$  and in  $a^2$  with  $\chi/(dof) = 1.1$ . The empty black circle is our result at the physical  $u/d$  quark mass point in the continuum limit. In this example we have considered  $\gamma = 0.75$ .

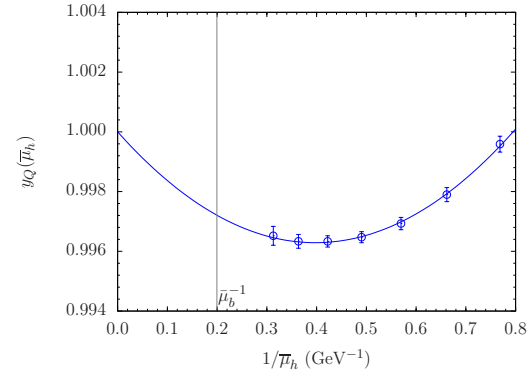


Figure 7:  $y_Q(\bar{\mu}_h)$  against  $1/\bar{\mu}_h$  using the fit ansatz of Eq. (17) with  $\chi^2/(dof) = 0.1$ . We have used  $\gamma = 0.75$ ,  $\lambda = 1.1588$  and  $\Lambda_{\overline{\text{MS}}}^{N_f=4} = 296(15)$  MeV for the running coupling entering in the  $\rho(\bar{\mu}_h, \mu)$  function. The vertical black thin line marks the position of  $1/\bar{\mu}_b$ . Quark mass values,  $\bar{\mu}_h, \bar{\mu}_b$  are expressed in the  $\overline{\text{MS}}$ -scheme at the scale of 2 GeV.

### References

- [1] FLAG, Aoki, S., et al., Eur.Phys.J. C74 (9) (2014) 2890. arXiv:1310.8555, doi:10.1140/epjc/s10052-014-2890-7.
- [2] S. Borsanyi, et al. arXiv:1406.4088.
- [3] Belle, Zupanc, A., et al., JHEP 1309 (2013) 139. arXiv:1307.6240, doi:10.1007/JHEP09(2013)139.
- [4] BaBar, del Amo Sanchez, P., et al., Phys.Rev. D82 (2010) 091103. arXiv:1008.4080, doi:10.1103/PhysRevD.82.091103.
- [5] CLEO-C, Naik, P., et al., Phys.Rev. D80 (2009) 112004. arXiv:0910.3602, doi:10.1103/PhysRevD.80.112004.



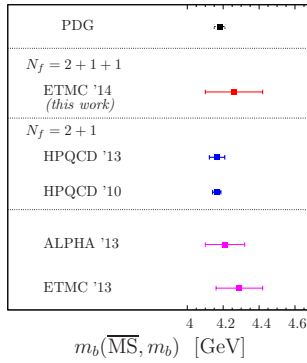


Figure 8: We compare the available continuum limit determinations for  $m_b(m_b)$  (in GeV) from lattice studies with  $N_f = 2, 2+1$  and  $2+1+1$  dynamical flavours. “ETMC ‘14” result refers to the present work. For the results of other lattice studies we refer to (from top to bottom) [42, 43, 44, 30]. For the PDG value see [31].

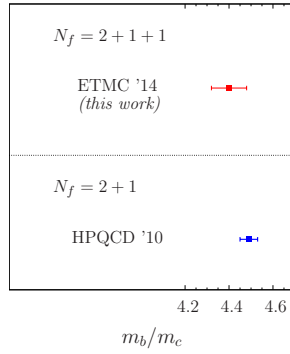


Figure 9: Comparison between the two available continuum limit determinations for  $m_b/m_c$  obtained from fully non-perturbative studies. For the “HPQCD” result see [43].

- [6] H.-B. Li, EPJ Web Conf. 72 (2014) 00011. doi:10.1051/epjconf/20147200011.
- [7] Y. Zheng, ICHEP 2014, these proceedings.
- [8] A. Djouadi, Phys.Rept. 457 (2008) 1–216. arXiv:hep-ph/0503172, doi:10.1016/j.physrep.2007.10.004.
- [9] ETMC, Carrasco, N., et al., Nucl.Phys. B887 (2014) 19–68. arXiv:1403.4504, doi:10.1016/j.nuclphysb.2014.07.025.
- [10] ETMC, Carrasco, N., et al., PoS (LATTICE 2013) (2013) 313. arXiv:1311.2837.
- [11] ETMC, Baron, R., et al., JHEP 1006 (2010) 111. arXiv:1004.5284, doi:10.1007/JHEP06(2010)111.
- [12] Y. Iwasaki, Nucl.Phys. B258 (1985) 141–156. doi:10.1016/0550-3213(85)90606-6.
- [13] R. Frezzotti, G. Rossi, Nucl.Phys.Proc.Suppl. 128 (2004) 193–202. arXiv:hep-lat/0311008, doi:10.1016/S0920-5632(03)02477-0.
- [14] ETMC, Baron, R., et al., Comput.Phys.Comm. 182 (2011) 299–316. arXiv:1005.2042, doi:10.1016/j.cpc.2010.10.004.
- [15] K. Osterwalder, E. Seiler, Annals Phys. 110 (1978) 440. doi:10.1016/0003-4916(78)90039-8.

- [16] S. Gusken, Nucl.Phys.Proc.Suppl. 17 (1990) 361–364. doi:10.1016/0920-5632(90)90273-W.
- [17] K. Jansen, et al., JHEP 0812 (2008) 058. arXiv:0810.1843, doi:10.1088/1126-6708/2008/12/058.
- [18] M. Albanese, et al., Phys.Lett. B192 (1987) 163–169. doi:10.1016/0370-2693(87)91160-9.
- [19] ETMC, Dimopoulos, P., et al. PoS(LATTICE 2013) (2013) 314. arXiv:1311.3080.
- [20] ETMC, Carrasco, N., et al. *in preparation*.
- [21] R. Frezzotti, G. C. Rossi, JHEP 08 (2004) 007. arXiv:hep-lat/0306014.
- [22] R. Frezzotti, et al., JHEP 0604 (2006) 038. arXiv:hep-lat/0503034, doi:10.1088/1126-6708/2006/04/038.
- [23] P. Dimopoulos, et al., Phys.Rev. D81 (2010) 034509. arXiv:0908.0451, doi:10.1103/PhysRevD.81.034509.
- [24] FNAL-MILC, Bazavov, A., et al. arXiv:1407.3772.
- [25]  $\chi$ QCD, Yang, Yi-Bo, et al. arXiv:1410.3343.
- [26] HPQCD, Na, Heechang, et al., Phys.Rev. D86 (2012) 054510. arXiv:1206.4936, doi:10.1103/PhysRevD.86.054510.
- [27] HPQCD, Davies, C.T.H., et al., Phys.Rev. D82 (2010) 114504. arXiv:1008.4018, doi:10.1103/PhysRevD.82.114504.
- [28] FNAL, Bazavov, A., et al., Phys.Rev. D85 (2012) 114506. arXiv:1112.3051, doi:10.1103/PhysRevD.85.114506.
- [29] ALPHA, Heitger, J., PoS LATTICE2013 (2013) 475. arXiv:1312.7693.
- [30] ETMC, Carrasco, N., et al., JHEP 1403 (2014) 016. arXiv:1308.1851, doi:10.1007/JHEP03(2014)016.
- [31] PDG, Olive, K.A., et al., Review of Particle Physics, Chin.Phys. C38 (2014) 090001. doi:10.1088/1674-1137/38/9/090001.
- [32] D. Becirevic, S. Fajfer, S. Pelovsek, J. Zupan, Phys.Lett. B563 (2003) 150–156. arXiv:hep-ph/0211271, doi:10.1016/S0370-2693(03)00653-1.
- [33] ETMC, Blossier, B., et al., JHEP 0907 (2009) 043. arXiv:0904.0954, doi:10.1088/1126-6708/2009/07/043.
- [34] G. Colangelo, et al., Nucl.Phys. B721 (2005) 136–174. arXiv:hep-lat/0503014, doi:10.1016/j.nuclphysb.2005.05.015.
- [35] S. Narison, Phys.Lett. B718 (2013) 1321–1333. arXiv:1209.2023, doi:10.1016/j.physletb.2012.10.057.
- [36] W. Lucha, D. Melikhov, S. Simula, Phys.Lett. B701 (2011) 82–88. arXiv:1101.5986, doi:10.1016/j.physletb.2011.05.031.
- [37] Z.-G. Wang, JHEP 1310 (2013) 208. arXiv:1301.1399, doi:10.1007/JHEP10(2013)208.
- [38] P. Gelhausen, et al., Phys.Rev. D88 (1) (2013) 014015. arXiv:1305.5432, doi:10.1103/PhysRevD.88.014015.
- [39] ETMC, Blossier, B., et al., JHEP 1004 (2010) 049. arXiv:0909.3187, doi:10.1007/JHEP04(2010)049.
- [40] ETMC, Dimopoulos, P., et al., JHEP 1201 (2012) 046. arXiv:1107.1441, doi:10.1007/JHEP01(2012)046.
- [41] K. Chetyrkin, et al., Phys.Rev. D80 (2009) 074010. arXiv:0907.2110, doi:10.1103/PhysRevD.80.074010.
- [42] HPQCD, Lee, A.J., et al., Phys.Rev. D87 (7) (2013) 074018. arXiv:1302.3739, doi:10.1103/PhysRevD.87.074018.
- [43] HPQCD, McNeile, C., et al., Phys.Rev. D82 (2010) 034512. arXiv:1004.4285, doi:10.1103/PhysRevD.82.034512.
- [44] ALPHA, Bernardoni, F., et al., Phys.Lett. B730 (2014) 171–177. arXiv:1311.5498, doi:10.1016/j.physletb.2014.01.046.